06

Anisotropy of two-photon absorption and Raman generation in $Na_2Mo_2O_7$ crystal

© D.S. Chunaev,[1] S.B. Kravtsov,[1] V.E. Shukshin,[1] V.N. Shlegel,[2] V.D. Grigorieva,[2] P.G. Zverev[1]

[1] Prokhorov General Physics Institute, Russian Academy of Sciences, Moscow, Russia
[2] Nikolaev Institute of Inorganic Chemistry, Siberian Branch, Russian Academy of Sciences, Novosibirsk, Russia

e-mail: zverev@lst.gpi.ru

Received December 12, 2024
Revised January 20, 2025
Accepted February 28, 2025

Two-photon absorption and stimulated Raman scattering in $Na_2Mo_2O_7$ crystal were studied when irradiated with picosecond laser pulses with a duration of 25 ps. The anisotropy of nonlinear optical properties and width of a band gap in the crystal is revealed. The maximum two-photon absorption coefficient at a wavelength of 523.5 nm was 7.8 cm/GW for radiation with a polarization parallel to the crystallographic axis **a**. Stimulated Raman scattering in $Na_2Mo_2O_7$ crystal with a Stokes shift of 939 cm^{-1} when pumped with a wavelength of 523.5 nm was obtained only when excited by radiation with a polarization parallel to the crystallographic axes **b** and **c** with Raman gain up to 10.3 cm/GW. The absence of stimulated Raman scattering when excited by radiation with a polarization parallel to axis **a**, which corresponds to maximal Raman gain coefficient, is due the competition of processes of the stimulated Raman scattering and the two-photon absorption

Keywords: Sodium dimolybdate, two-photon absorption, band gap, stimulated raman scattering.

DOI: 10.61011/EOS.2025.03.61157.9-25

Introduction

The search for nonlinear crystals for efficient solid-state converters of laser radiation based on stimulated Raman scattering (SRS) is an urgent task of modern laser physics. SRS makes it possible to convert laser radiation from well-developed lasers into new spectral wavelength ranges and to create compact and reliable laser radiation sources [1–3]. High radiation intensity is required to reach the SRS threshold, which may lead to other nonlinear processes including two-photon absorption, self-focusing [4,5]. Two-photon absorption (TPA) limits the use of SRS converters in the visible and near-ultraviolet regions of the spectrum, when the operating wavelength is close to the fundamental absorption edge in the medium [6,7].

The transparency of the optical medium in the visible and near-ultraviolet ranges is determined by the width of the band gap E_g, which is determined by the energy gap between the bottom of the conduction band and the upper levels of the valence band. Most of the SRS-active materials based on oxide molecular-ion complexes have the energy width of the band gap 3–6 eV [8,9]. Irradiation of the medium with intense light with photon energy exceeding half E_g can lead to two-photon interband transitions. TPA creates long-lived optical centers that lead to single-photon absorption of excitation radiation and reduce its intensity.

Recently, the technology for producing crystals of sodium dimolybdate $Na_2Mo_2O_7$ has been improved and it has become possible to obtain samples of this crystal with a high optical quality [10]. $Na_2Mo_2O_7$ crystal exhibits strong anisotropy of optical properties. It has been recently shown that $Na_2Mo_2O_7$ has intense lines in the Raman spectrum and is a highly efficient SRS-active material. Its Raman gain at the optimal orientation is 12.4 cm/GW at wavelength of 1.047 μm, which is one of the highest values for solid-state SRS-active media [11].

The aim of this paper was to study the anisotropy of nonlinear TPA of 523.5 nm radiation in $Na_2Mo_2O_7$ crystal, to obtain SRS generation in it under excitation by picosecond laser pulses, and to analyze the impact of TPA on the SRS generation process depending on the polarization of pumping radiation.

Experimental sample of $Na_2Mo_2O_7$ crystal

$Na_2Mo_2O_7$ crystal has an orthorhombic structure with lattice cell parameters $a = 7.2$ Å, $b = 11.8$ Å, $c = 14.7$ Å. The studied crystal sample was grown using the Czochralski method in a platinum crucible; details of the growth process are described in Ref. [10]. The experimental crystal sample was cut along the crystallographic axes **a**, **b**, and **c** in the form of a rectangular parallelepiped with polished faces and had dimensions $7.3 \times 6.0 \times 3.5$ mm. $Na_2Mo_2O_7$ crystal is transparent in the visible and near-infrared spectral ranges up to wavelength of 5 μm [10]. The short-wave transmittance edge of the crystal lies around the wavelength of 370 nm.

So far, the transparency of crystals in the ultraviolet region of the spectrum has been studied only for unpolarized radiation [12]. Cary-5000 spectrometer (Varian) operating in

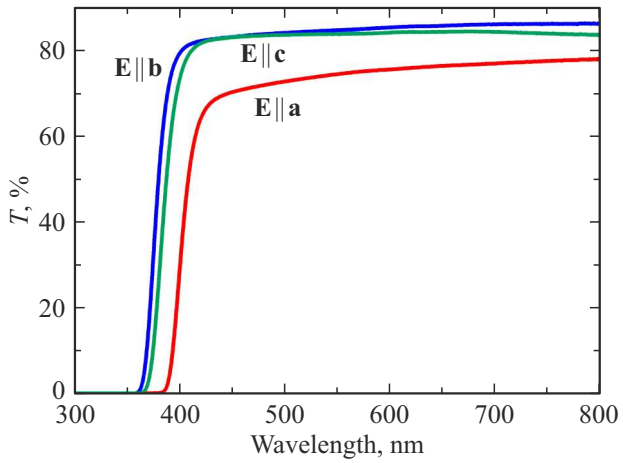

Figure 1. Polarized transmission spectra of the sample of $Na_2Mo_2O_7$ crystal.

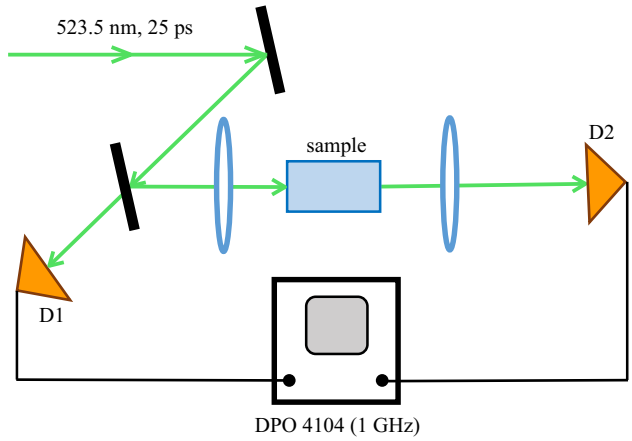

Figure 2. Schematic diagram of the experimental setup for measuring the TPA coefficient in $Na_2Mo_2O_7$ crystal.

the spectral range 175−3200 nm with a spectral resolution of 0.08 nm and Glan-Taylor polarizers were used in our experiments to obtain polarized transmission spectra. Fig. 1 shows the polarized transmission spectra of $Na_2Mo_2O_7$ crystal for polarizations parallel to all three crystallographic axes **a**, **b**, and **c**. It can be seen that the transmission spectrum of the crystal strongly depends on the orientation of the crystal. The ultraviolet transmission boundary is located in the region of 365−370 nm for the radiation polarizations **E** ∥ **b** and **E** ∥ **c** , and it is shifted towards the red region for **E** ∥ **a** and is near the wavelength of 390 nm. It should be noted that the transmittance of the sample in the visible region of the spectrum for this polarization is 73%, which is noticeably less than the transmittance for polarizations **E** ∥ **b** and **E** ∥ **c**, equal to 84%. This is due to the difference in the magnitude of the Fresnel reflection for different crystal orientations and indicates a higher value of the refractive index for the polarization **E** ∥ **a**.

Anisotropy of two-photon absorption coefficient in $Na_2Mo_2O_7$ crystal

The values of TPA coefficients in $Na_2Mo_2O_7$ crystal for different light polarizations were measured at a wavelength of 523.5 nm using the express technique proposed in Ref. [9]. The experiment measures the sample's transmittance of a train of picosecond laser pulses with smoothly varying amplitude passes through it. A pulsed neodymium laser with a Nd:YLF crystal with passive mode locking, which gives polarized radiation at a wavelength of 1047 nm, was used as a radiation source. The second harmonic generation at 523.5 nm was achieved using a frequency doubler with a $LiIO_3$ nonlinear crystal. The laser generated trains of picosecond pulses, with their duration measured using an Imacon-501 streak camera and determined to be 25 ps FWHM. The maximum energy of the laser pulse train was about 1.5 mJ. The second harmonic radiation was focused by a lens ($f = 250$ mm) into the studied sample. The transverse intensity profile of the laser radiation followed a Gaussian distribution, with the measured second harmonic beam waist radius at the lens focus (intensity level $1/e^2$) being $\omega_0 = 73\,\mu$m. The Gaussian beam's waist effective length was approximately 30 mm, significantly exceeding the sample dimensions, thus allowing the laser beam's cross-sectional area within the sample to be considered as constant. Calibrated silicon photodiodes D_1 and D_2 and Tektronix DPO4104 oscilloscope (Fig. 2) were used to measure the energy of individual picosecond pulses of incident and transmitted radiation. For a pump beam radius at the focus of $\omega_0 = 73\,\mu$m, a pulse train duration of 25 ps, and single pulse energy up to 1 μJ, the pump radiation power density in the sample reached 0.5 GW/cm^2.

The intensity change I of light along the propagation axis z is determined using following equation in case of TPA [13]

$$\frac{dI}{dz} = -\alpha I - \beta I^2 \tag{1}$$

where α is the linear absorption coefficient, β is the TPA coefficient. The equation (1) is solved as follows in the case of the absence of the linear absorption $\alpha = 0$:

$$I(z) = \frac{I_0}{1 + \beta z I_0}, \tag{2}$$

where I_0 is the light intensity at $z = 0$. Then the attenuation of light passing through the medium of length L is expressed by the relation

$$\frac{I_0}{I(L)} = 1 + \beta L I_0. \tag{3}$$

For pulsed radiation with a Gaussian time profile and a pump beam with a Gaussian transverse distribution, equation (3) is transformed into an expression for the energy attenuation of light as a function of the pulse energy at the entrance to the sample E_{in}:

$$\frac{E_{in}}{E_{out}} = \frac{1}{T_{in}T_{out}}\left(1 + \beta L \frac{1}{2\sqrt{2}}\frac{1}{\tau}\frac{T_{in}E_{in}}{\frac{1}{2}\pi\omega_0^2}\right). \tag{4}$$

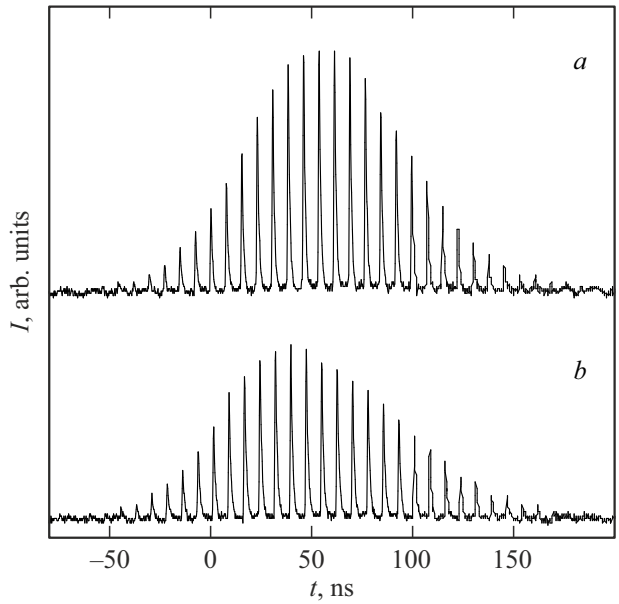

Figure 3. Pulse trains of (a) incident and (b) transmitted radiation through $Na_2Mo_2O_7$ crystal, with a wavelength of 523.5 nm and polarization **E** || **a**.

Here E_{out} is the pulse energy after passing the sample, T_{in} and T_{out} are the transmission coefficients associated with Fresnel reflection at the entrance and exit of the crystal sample, ω_0 is the beam radius at level $1/e^2$, and τ is the effective pulse duration, which is equal to

$$\tau = \frac{\tau_{1/2}}{\sqrt{\ln 2}} \frac{\sqrt{\pi}}{2}, \qquad (5)$$

where $\tau_{1/2}$ is the FWHM pulse duration.

It can be seen from (4) that the energy attenuation at TPA increases linearly with the increase of energy E_{in} of the incident radiation. The dependence is a straight line with the slope equal to

$$B = \beta L \frac{1}{2\sqrt{2}} \frac{1}{\tau} \frac{1}{\frac{1}{2}\pi\omega_0^2} T_{in}. \qquad (6)$$

The value of the TPA coefficient β can be determined from equation (6) by determining the slope of the experimental dependence B.

523.5 nm radiation falls within the transparency range of $Na_2Mo_2O_7$ crystal, and the doubled energy of the quantum falls within the fundamental absorption region. The TPA efficiency in $Na_2Mo_2O_7$ will depend on the polarization of the radiation due to the anisotropy of the crystal. The experimental oscillograms of pulse trains incident on the crystal and passing through it for radiation with polarization **E** || **a** are shown in Fig. 3. The laser emits a train of picosecond pulses in a single flash with a smoothly varying intensity corresponding to the energy in the individual pulses. Since the duration of picosecond pulses in a train and their transverse size are constant, the entire energy dependence for the nonlinear process can be measured in a single laser flash. Fig. 4, a shows the experimental dependence of the light attenuation for individual pulses from the train presented in Fig. 3 for polarization **E** || **a** on the incident pulse energy E_{in} in the range up to 1 μJ. It can be seen that a linear increase of the attenuation of radiation due to TPA is observed at the beginning of the train with the increase of energy E_{in}. For subsequent pulses, further attenuation is observed, related to residual single-photon absorption at induced long-lived optical centers and independent of the intensity of individual pulses. The number of induced optical centers depended on the efficiency of the TPA process. The lifetime of the induced centers depends on the sample material and can reach several seconds [14]. The experimental energy attenuation dependence of the incident pulse energy E_{in} in the range up to 12 μJ for the radiation polarization **E** || **c** is shown in Fig. 4, b. It can be seen that the slope of this dependence is much lower than for the polarization **E** || **a**, which is attributable to the smaller value of the TPA coefficient.

The values of the slope B of the experimental dependencies for different orientations of the sample and the calculated values of the TPA coefficient β are given in Table 1. It can be seen that the nonlinear TPA coefficient for polarization **E** || **a** is almost one and a half orders of magnitude larger than the TPA coefficient for polarizations **E** || **b** and **E** || **c**. This dependence is related to the shift of the fundamental absorption boundary in $Na_2Mo_2O_7$ for polarization **E** || **a** to the red region, which is attributable to the strong anisotropy of the fundamental absorption in it.

The crystal structure and electronic states of atoms in $Na_2Mo_2O_7$ crystal using first principles was studied in Ref. [15]. The authors showed that the low-energy conduction band levels that define the fundamental absorption boundary are associated with electronic transitions of 4d-electrons in molybdenum atoms and 2p-electrons in oxygen atoms. Calculations showed that the width of the band gap E_g is 2.87 eV, while the experimentally measured band gap width was 3.69 eV [10]. Such a discrepancy of values E_g may be attributable to the fact that the authors of these papers did not take into account the strong anisotropy of electronic states in the conduction zone and valence band, which determine the fundamental absorption boundary and the TPA coefficient.

Influence of two-photon absorption process on SRS generation in $Na_2Mo_2O_7$ crystal

Molybdate crystals are known as high-efficiency materials for SRS [16], and molybdates activated by rare-earth ions can be both active and nonlinear medium of a laser with SRS self-converted emission [2]. The SRS of light is usually obtained at the most intense modes in the spontaneous Raman scattering spectrum of the medium. This mode

Table 1. The values of the TPA coefficients β at wavelength 523.5 nm and the slope of the experimental light attenuation dependence B for different orientations of $Na_2Mo_2O_7$ crystal

Polarization of radiation	Direction of propagation of radiation	Length of sample, mm	Slope of light attenuation B, $1/\mu$J	Coefficient of TPA β, cm/GW
E ∥ **a**	**k** ∥ **b** **k** ∥ **c**	6.0 3.5	0.66 0.46	6.7 ± 1.0 7.8 ± 1.0
E ∥ **b**	**k** ∥ **c** **k** ∥ **a**	3.5 7.3	0.01 0.025	0.17 ± 0.02 0.2 ± 0.02
E ∥ **c**	**k** ∥ **a** **k** ∥ **b**	7.3 6.0	0.015 0.013	0.12 ± 0.02 0.13 ± 0.02

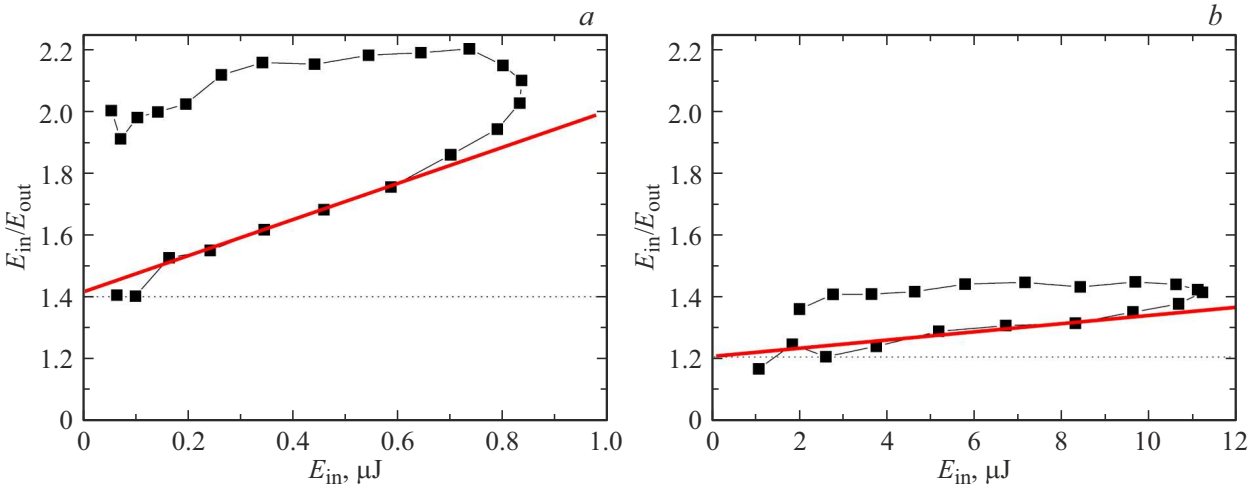

Figure 4. The dependence of light attenuation in $Na_2Mo_2O_7$ crystal on the incident energy for radiation passing through the sample along the axis **b** with polarization **E** ∥ **a** (*a*) and **E** ∥ **c** (*b*).

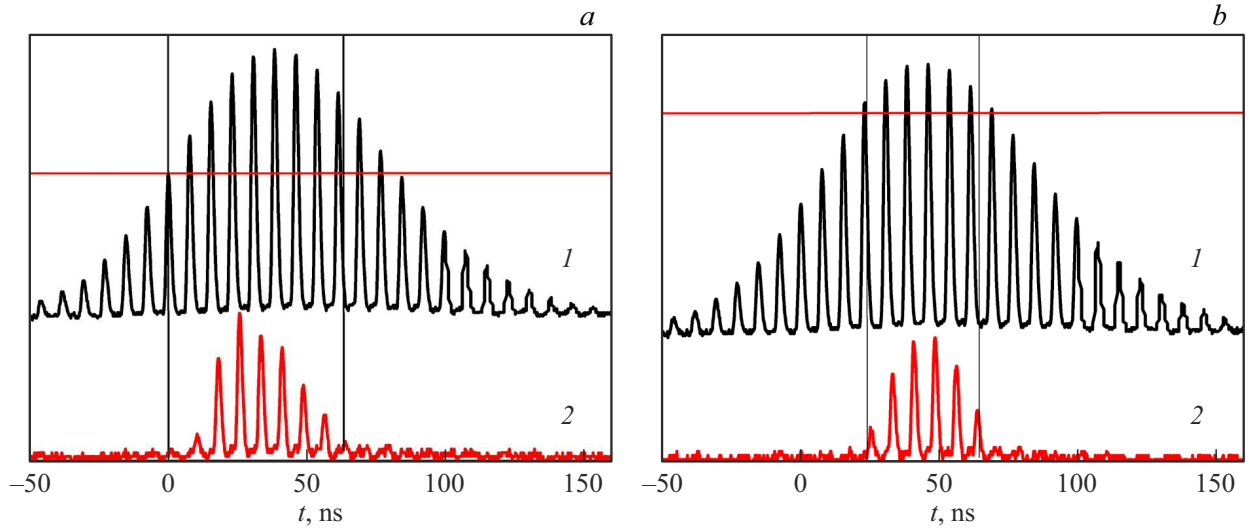

Figure 5. Trains of pumping pulse (1) and SRS generation (2) in $Na_2Mo_2O_7$ crystal with a length of 7.3 mm and pumping polarization **E** ∥ **b** (*a*) and in KGW crystal with a length of 10 mm and pumping polarization **E** ∥ **m** (*b*). Details in the text.

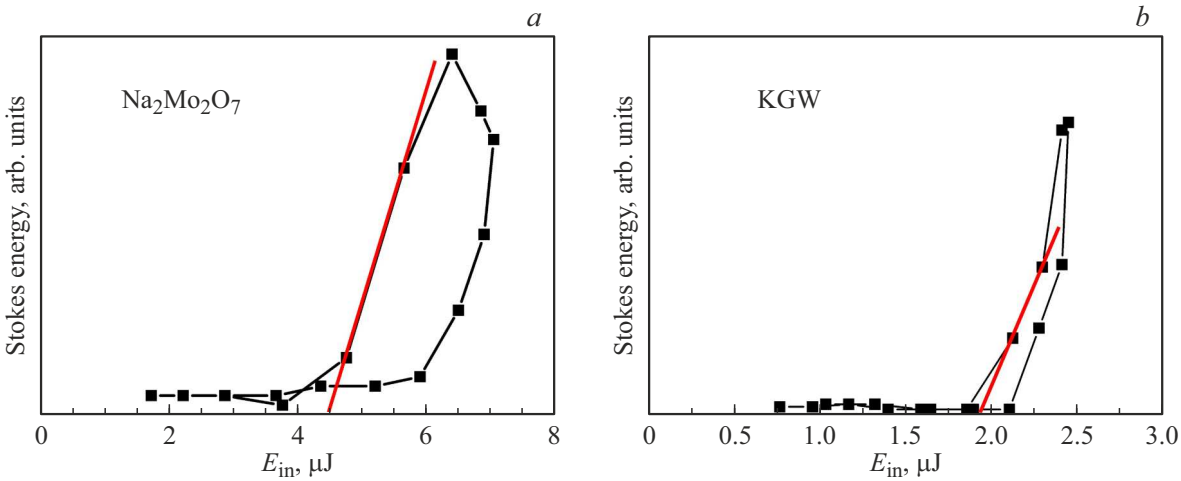

Figure 6. Dependences of the energy of SRS pulses on the energy of excitation radiation pulses in a train in $Na_2Mo_2O_7$ crystal of length 7.3 mm for the pumping radiation polarization **E** ∥ **b** (*a*) and in the KGW crystal with a length of 10 mm for the radiation polarization **E** ∥ **m** (*b*).

Table 2. Threshold, normalized threshold and Raman gain in $Na_2Mo_2O_7$ and KGW crystals for different sample orientations

Polarization of radiation	Direction of beam	Length of sample,mm	Threshold, μJ	Normalized threshold, $L = 1$ cm, μJ·cm	Raman gain, cm/GW
$Na_2Mo_2O_7$					
E ∥ **c**	**k** ∥ **a**	7.3	4.0 ± 0.3	2.9	8.2 ± 1.0
E ∥ **c**	**k** ∥ **b**	6.0	4.6 ± 0.3	2.8	8.5 ± 1.0
E ∥ **b**	**k** ∥ **a**	7.3	4.0 ± 0.3	2.9	8.2 ± 1.0
E ∥ **b**	**k** ∥ **c**	3.5	6.5 ± 0.3	2.3	10.3 ± 1.5
KGW					
E ∥ **m**	**k** ∥ **g**	10	1.9 ± 0.1	1.9	12.5 ± 1.5

corresponds to the valence bond vibrations of Mo^{6+} ion and O^{2-} ions in $Na_2Mo_2O_7$ crystal [12] with the frequency of 939 cm^{-1}. The highest intensity of this line is observed when the radiation propagates along the crystallographic axes **b** or **c** and is polarized along the axis **a** [11]. The ratio of intensities of 939 cm^{-1} lines in the Raman spectrum for other orientations gives a ratio of the scattering tensor components of about three, which implies a threefold smaller scattering cross section and, correspondingly, a threefold higher SRS threshold.

We first observed SRS in $Na_2Mo_2O_7$ crystal in this study in case of the excitation by picosecond laser pulses with a wavelength of 523.5 nm. The experimental setup described above was used, only in the output stage a diffraction grating was used for spectral selection of radiation at the wavelength of the first Stokes component, which was 550 nm. Tighter focusing with $f = 150$ mm lens was used to achieve the SRS threshold. In this case, the beam waist diameter of the second harmonic radiation decreased to $\omega_0 = 41\,\mu$m at the level $1/e^2$ from the intensity maximum, which allowed for a pulse with energy $E = 1\,\mu$J to increase the power density at the focus to $I = 1.4$ GW/cm^2. The energy of individual picosecond pulses in the pump and scattered radiation train was measured during a single laser flash using a digital oscilloscope (Fig. 5), and the dependence of the SRS efficiency on the pump pulse energy was determined. A technique for measuring the Raman gain factor in a sample by comparing the energy thresholds of SRS occurrence with a known crystal is described in Ref. [16].

We measured the Raman gain by comparing the SRS occurrence thresholds in $Na_2Mo_2O_7$ and in a well-known high-performance SRS-active potassium-gadolinium tungstate (KGW) crystal (Table 2). SRS in the KGW crystal was excited along the optical indicatrix g axis, the interaction length in the sample was 1 cm. When the SRS is excited by radiation with polarization parallel to the axis **m**, the SRS with a Stokes shift of 901 cm^{-1} is generated [17]. Fig. 5 shows the experimental trains of picosecond excitation pulses and SRS pulses in $Na_2Mo_2O_7$ crystal for the pumping

radiation polarization $\mathbf{E} \parallel \mathbf{b}$ and in the KGW crystal for $\mathbf{E} \parallel \mathbf{m}$. The threshold for the occurrence of SRS is clearly visible (horizontal line). It is necessary to note that the train of SRS pulses in KGW is symmetrically located with respect to the pumping train, while in $Na_2Mo_2O_7$ it is shifted to the beginning of the pumping train. This is attributable to the fact that an induced absorption occurs in $Na_2Mo_2O_7$ crystal in the high energy train pulses due to TPA, which reduces the intensity of the transmitted radiation and the efficiency of SRS at the final part of the train. The trains are symmetrical in the KGW crystal because it does not have the TPA at wavelength 523.5 nm, since its band gap width is much larger and is 3.9–4.51 eV [18].

The spectral width of the SRS-active mode in $Na_2Mo_2O_7$ and KGW crystals is 3.5 and 5.4 cm^{-1}, which corresponds to mode dephasing time T_2 equal to 3 and 2 ps respectively [11,16]. Since the effective duration of the pumping pulse τ in our experiments is much longer than the dephasing time, the SRS generation mode can be considered stationary. In this case, under conditions of small Stokes signals and undepleted pumping, the increment of the SRS amplification G is proportional to the pumping intensity I and the length of the nonlinear interaction L:

$$G = gIL, \tag{7}$$

where g is the steady-state Raman gain in the medium. It follows from equation (7) that, assuming a Gaussian spatial and temporal distribution of the pump radiation, the threshold value of the increment G_{thr}, equal to 25, is reached at the threshold energy of the pulses in the train

$$G_{\text{thr}} = 25 = gLE_{\text{thr}} \frac{1}{2\sqrt{2}} \frac{1}{\tau} \frac{1}{\frac{1}{2}\pi\omega_0^2}. \tag{8}$$

Here E_{thr} is the threshold energy of the picosecond pulse, τ is the effective pulse duration according to Equation (5), ω_0 is the pumping beam radius at level $1/e^2$.

Fig. 6 shows the dependences of the energy of the SRS pulses on the energy of the excitation radiation pulses. It can be seen that the dependence has the appearance of hysteresis in $Na_2Mo_2O_7$ due to the accompanying TPA. The linear approximation of the initial section of the SRS-generation train gives us the opportunity to determine the value of the energy threshold of SRS, calculate the threshold given by 1 cm of the nonlinear medium, and determine the steady-state Raman gain using (8). The SRS threshold in a 10 mm long KGW crystal was about 1.9 μJ in our experiments. The SRS threshold for $Na_2Mo_2O_7$ crystal was slightly higher and ranged from 4 to 6.5 μJ. The present threshold was also higher and amounted to 2.3–2.9 μJ·cm, which was associated with a smaller value of the steady-state Raman gain, which ranged from 8.2 to 10.3 cm/GW. These values are slightly lower than in the KGW crystal, which requires higher pumping energy to obtain efficient SRS generation. It should be noted that the maximum value of the Raman gain was observed in the sample of minimum length, which may be attributable to the lack of competition with TPA at shorter sample length.

The SRS in $Na_2Mo_2O_7$ crystal under excitation by 1.047 μm radiation was studied in Ref. [11]. It was found that the maximum Raman gain in $Na_2Mo_2O_7$ is observed for the polarization $\mathbf{E} \parallel \mathbf{a}$, which corresponds to the geometry of the maximum spontaneous Raman scattering cross section in the crystal. Moreover, in this case, the Raman amplification is about three times higher than for polarizations $\mathbf{E} \parallel \mathbf{b}$ and $\mathbf{E} \parallel \mathbf{c}$. The SRS amplification for the polarization $\mathbf{E} \parallel \mathbf{a}$ should be about 30 cm/GW for a 523.5 nm pumping. However, no SRS generation was observed in the experiment when pumped with radiation with polarization $\mathbf{E} \parallel \mathbf{a}$. This is because very strong TPA is observed for radiation with this polarization, which leads to the formation of induced absorption that absorbs a significant fraction of the excitation radiation.

Conclusion

The anisotropy of TPA and SRS in $Na_2Mo_2O_7$ crystal excited by laser pulses at a wavelength of 523.5 nm and duration of 25 ps has been studied. Anisotropy of the band gap width in the crystal is revealed. This leads to a strong anisotropy of the TPA coefficient, which at a wavelength of 523.5 nm was 7.8 cm/GW for radiation with polarization $\mathbf{E} \parallel \mathbf{a}$ and 0.12 – 0.2 cm/GW for polarizations $\mathbf{E} \parallel \mathbf{b}$ and $\mathbf{E} \parallel \mathbf{c}$. SRS generation has been first obtained on $Na_2Mo_2O_7$ crystal excited by 523.5 nm radiation with a Stokes shift of 939 cm^{-1}, which provides emission at a wavelength of 550 nm. In accordance with the spectrum of spontaneous Raman scattering, the maximum SRS-amplification coefficient in the crystal is observed for the polarization $\mathbf{E} \parallel \mathbf{a}$, which, when excited by 523.5 nm radiation is suppressed by induced losses due to TPA. The measured steady-state Raman gain ranged from 8.2 to 10.3 cm/GW for excitation radiation with polarizations $\mathbf{E} \parallel \mathbf{b}$ and $\mathbf{E} \parallel \mathbf{c}$, which is comparable to KGW crystal.

The studies have shown that $Na_2Mo_2O_7$ crystal is a promising nonlinear optical medium with strong anisotropy of the crystal structure, which should be taken into account when creating devices based on it.

Conflict of interest

The authors declare that they have no conflict of interest.

References

[1] T.T. Basiev, R.C. Powell. *Solid-state Raman lasers*. In: *Handbook of Laser Technology and Applications* (CRC Press, 2021), p. 127–149. DOI: 10.1201/9781003127130

[2] H. Zhao, S. Dai, S. Zhu, H. Yin, Z. Li, Z. Chen. Crystals, **11**, 114 (2021). DOI: 10.3390/cryst11020114

[3] P. Cerny, H. Jelinkova, P.G. Zverev, T.T. Basiev. Progr. Quant. Electron., **28**, 113 (2004). DOI: 10.1016/j.pquantelec.2003.09.003

[4] M. Rumi, J.W. Perry. Adv. Opt. Photon., **2**, 451 (2010). DOI: 10.1364/AOP.2.000451
[5] D.N. Christodoulides, I.C. Khoo, G.J. Salamo, G.I. Stegeman, E.W. Van Stryland. Adv. Opt. Photon., **2**, 60 (2010). DOI: 10.1364/AOP.2.000060
[6] P. Jiang, X. Ding, J. Guo, H. Zhang, H. Qi, Y. Shang, Z. Song, W. Wang, C. Wang, G. Liu, C. Yao. Opt. Laser Tech., **169**, 110072, (2024). DOI:
[7] I.O. Kinyaevskiy, V.I. Kovalev, A.V. Koribut, E.E. Dunaeva, N.S. Semin, A.A. Ionin. Opt. Spectrosc., **131** (2), 196 (2023). DOI: 10.61011/EOS.2023.02.55785.8-23
[8] R. Lacomba-Perales, J. Ruiz-Fuertes, D. Errandonea, D. Martínez-García, A. Segura. Europhys. Lett., **83**, 37002 (2008). DOI: 10.1209/0295-5075/83/37002
[9] V.I. Lukanin, D.S. Chunaev, A.Y. Karasik. J. Exp. Theor. Phys., **113**, 412 (2011). DOI: 10.1134/S1063776111070077.
[10] V.D. Grigorieva, V.N. Shlegel, N.V. Ivannikova, T.B. Bekker, A.P. Yelisseyev, A.B. Kuznetsov. J. Crystal Growth, **507**, 31 (2019). DOI 10.1016/j.jcrysgro.2018.10.058
[11] D.S. Chunaev, S.B. Kravtsov, V.E. Shukshin, V.N. Shlegel, V.D. Grigorieva, P.G. Zverev. Bulletin of the Lebedev Physics Institute, **51**, 11, S919–S927 (2024). DOI: 10.3103/S1068335624602796.
[12] D.A. Spassky, N.S. Kozlova, M.G. Brik, V. Nagirnyi, S. Omelkov, O.A. Buzanov, M. Buryi, V. Laguta, V.N. Shlegel, N.V. Ivannikova. J. Lumin., **192**, 1264 (2017). DOI: 10.1016/j.jlumin.2017.09.006
[13] A. Dragomir, J.G. McInerney, D.N. Nikogosyan. Appl. Opt. **41** (21), 4365 (2002). DOI: 10.1364/AO.41.004365
[14] V.I. Lukanin, A.Y. Karasik. Opt. Spectrosc., **121** 503 (2016). DOI: 10.1134/S0030400X16100143.
[15] Y. Gao, C. Zhang, L. Ma, H. Li, S. Chen. Phys. Stat. Sol. B, **259** (8), 2200036 (2022). DOI: 10.1002/pssb.202200036
[16] T.T. Basiev, P.G. Zverev, A.Y. Karasik, V.V. Osiko, A.A. Sobol', D.S. Chunaev. J. Exp. Theor. Phys., **99**, 934 (2004). DOI: 10.1134/1.1842874.
[17] I.V. Mochalov. Opt. Engineer., **36**, 1660 (1997). DOI: 10.1117/1.601185
[18] V.I. Lukanin, A.Y. Karasik. Opt. Commun., **336**, 207 (2015). DOI: 10.1016/j.optcom.2014.10.012

Translated by A.Akhtyamov